Over-expression of Bcl-2 does not protect cells from hypericin photo-induced mitochondrial membrane depolarization, but delays subsequent events in the apoptotic pathway

Roman Chaloupka[a,b], Patrice Xavier Petit[c], Nicole Israël[d], Franck Sureau[a,c,*]

[a] *Laboratoire de Physicochimie Biomoléculaire et Cellulaire (CNRS ESA 7033), Université P. et M. Curie, Case 138, 4 Place Jussieu, F-75252 Paris Cedex 05, France*
[b] *Institute of Physics, Charles University, Ke Karlovu 5, 12116 Prague, Czech Republic*
[c] *Unité de Recherche en Physiologie et Pathologie Génétiques et Moléculaires (INSERM U129), I.C.G.M., Faculté de médecine Cochin, Port Royal, 24 rue du Faubourg Saint-Jacques, 75014 Paris, France*
[d] *Unité de Biologie des Rétrovirus, Institut Pasteur, 28 rue du docteur Roux, 75724 Paris Cedex 15, France*

Received 24 August 1999; received in revised form 5 October 1999

Edited by Vladimir Skulachev

Abstract Hypericin (HY) is a powerful photo-inducer of apoptosis in Jurkat cells as measured by caspase-3 activation, cell shrinkage, phosphatidylserine (PS) exposure and the appearance of hypoploid DNA. These processes are preceded by rapid Bcl-2-independent mitochondrial transmembrane depolarization and a drop in cytoplasmic pH. Pre-incubation of cells with inhibitors of the mitochondrial permeability transition pore, such as cyclosporin A or bongkrekic acid, does not protect cells from mitochondrial membrane potential ($\Delta\psi_m$) decrease. However, monitoring of mitochondrial entrapped calcein by confocal fluorescence imaging gives clear evidence of HY photo-induced mitochondrial permeability. This should be considered as the result of a non-specific alteration of mitochondrial membrane integrity brought about by lipid peroxidation. Nevertheless, synthesis of the anti-apoptotic protein Bcl-2 appears to delay the subsequent time course of PS exposure and to reduce caspase-3 activation and the fraction of cells which become hypoploid. We interpret this partially protective effect as the consequence of a direct interaction of Bcl-2 with cytosolic cytochrome *c* previously released from mitochondria upon $\Delta\psi_m$ decrease and/or of Bcl-2 inhibition of the deleterious retro-effect of caspase-3 on the mitochondrial permeability transition pore and/or the mitochondrial membrane components.

© 1999 Federation of European Biochemical Societies.

Key words: Apoptosis; Bcl-2; Caspase; Cellular photosensitization; Cyclosporin A; Hypericin; Mitochondrial membrane potential

1. Introduction

Hypericin (HY) is a natural product structurally related to the perihydroxylated polycyclic quinones. HY is found in *Hypericum perforatum* and other plants of the same genus and has traditionally been used in occidental folk medicine [1]. HY displays light-dependent anti-viral activity against several types of enveloped viruses including HIV-1 and HSV-1 [2,3]. HY also causes oxygen-dependent cell phototoxicity and in vivo anti-tumor and preclinical evaluation have shown it to be a promising agent for the photodynamic therapy of cancer [4–7]. It has been shown that HY photosensitization inhibits protein kinase C [8,9], epidermal growth factor receptor, tyrosine kinase activity [10] and the activity of succinoxidase, a mitochondrial enzyme involved in the respiratory oxidation necessary for ATP formation [4]. The effect of HY on isolated rat liver mitochondria has been studied in more detail [11]. Both the respiratory control ratio and the mitochondrial membrane potential ($\Delta\psi_m$) were found to be decreased by HY photosensitization. Further evidence of the ability of HY to impair mitochondrial function in vitro was supplied by recent measurements of the bioenergetics (ATP content and respiratory activity) of EMT6 mouse mammary carcinoma cells. The authors suggest that 'one possible discrete target of HY phototoxicity may be mitochondria' [12]. The multiple actions of HY also involve an alteration of mitochondria-bound hexokinase, leading to a cascade of events that alter the energy metabolism and survival of glioma cells [13]. Following irradiation, the nuclear DNA fragmentation characteristic of apoptotic cells has been observed after long term exposure (24 h) of glioma cell lines to HY [14]. The release of cytochrome *c* from the mitochondrial membrane as well as procaspase-3 activation have recently been reported as a consequence of the HY-induced photosensitization of HeLa cells [15]. The breakdown of $\Delta\psi_m$ is currently believed to characterize the early stages of the apoptotic process: a stage which precedes cell shrinkage, nuclear disintegration and nuclear DNA fragmentation in a variety of cells. This disruption may involve a mitochondrial permeability transition leading to the uncoupling of oxidative phosphorylation and to the generation of superoxide anions [16]. Thus, mitochondria may be an important potential target of HY and account for its anti-neoplastic activity. From a mechanistic point of view, the formation of a singlet oxygen and/or superoxide anion radical (type II photosensitization) is generally considered to be responsible for the phototoxic effect [4], although a type I radical which generates hydroxyl radicals may also play a role [17]. We and others have suggested that 'an alternative origin for the photo-induced activity of HY may involve its ability to produce a photogenerated pH drop through an in-

*Corresponding author. Fax: (33)-1-44 27 75 60.
E-mail: sureau@lpbc.jussieu.fr

Abbreviations: HY, hypericin; $\Delta\psi_m$, mitochondrial membrane potential; PS, phosphatidylserine; CsA, cyclosporin A; $DiOC_6(3)$, 3,3′-dihexyloxacarbocyanine iodide; BCECF-AM, 2′,7′-bis(2-carboxyethyl)-5-(and 6)-carboxyfluorescein acetoxymethylester; FITC, fluorescein isothiocyanate; PI, propidium iodide; MPT, mitochondrial permeability transition; BA, bongkrekic acid

0014-5793/99/$20.00 © 1999 Federation of European Biochemical Societies. All rights reserved.
PII: S0014-5793(99)01538-0

tramolecular proton transfer in the excited state of the molecule, which is likely to precede its local environment acidification' [18]. Indeed, a photo-induced pH decrease to 6.8 has been observed in 3T3 cells incubated with HY or with the related compound hypocrellin A [19,20]. Such a local pH drop could be associated with the classical type I and II mechanisms for boosting the formation of highly reactive protonated oxygen species such as $HO_2^{\bullet}$ [21]. Interestingly, intracellular acidification has also been reported as an early event in apoptosis [22]. However, the cellular mechanism of HY phototoxicity remains unclear. We have now monitored the effects of HY photosensitization on $\Delta\psi_m$, caspase activation, phosphatidylserine (PS) exposure on the external leaflet of the plasma membrane and the emergence of hypoploidy in control and Bcl-2-transfected cells to characterize the apoptotic pathway and to evaluate the suitability of mitochondria as a pharmacological target of this compound. The protective effects of cyclosporin A (CsA) and bongkrekic acid (BA) were also tested.

2. Materials and methods

2.1. Chemicals

HY was obtained from Roth (Karlsruhe, Germany). HA was obtained from Molecular Probes (Eugene, OR, USA). Stock solutions were prepared in DMSO and stored in the dark at −20°C. Caspase-3 fluorescence detection kits and the fluorescent probes 3,3′-dihexyloxacarbocyanine iodide ($DiOC_6(3)$), 2′,7′-bis(2-carboxyethyl)-5-(and 6)-carboxyfluorescein acetoxymethylester (BCECF-AM) and propidium iodide (PI) were purchased from Molecular Probes (Eugene, OR, USA). The Annexin V-fluorescein isothiocyanate (FITC) kit was obtained from Coulter-Immunotech (Marseille, France). In some experiments, the ligand of the adenine nucleotide translocator, bongkrekic acid (50 μM final) or cyclosporin A (1 μM final) were added to HY-treated cells 15 min before irradiation. BA was kindly provided by Dr Duine (Delft University, Delft, The Netherlands) and CsA was purchased from Novartis (Switzerland).

2.2. Cell culture

The J Jhan human lymphoblastoid $CD4^+$ T-cell line (derived from the Jurkat cell line provided by JD Fox, London, UK) was grown in RPMI 1640 medium with 5% (v/v) fetal calf serum, 2 mM L-glutamine, penicillin (100 U/ml) and streptomycin (100 μg/ml) in 5% CO_2/95% humidified air at 37°C at a density of 10^6 cells per ml. J Jhan were transfected with CMV-s bcl-2 (JK-Bcl-2) or the control vector pcDNA3 (JKV) by an electroporation procedure and selected on G418 medium as previously described [23]. The flow cytometry analysis of Bcl-2 expression was performed using anti-bcl-2 fluorescent antibody labelling (Bcl-2 oncoprotein-FITC, DAKO clone 123) on 70% ethanol-fixed cells. Western blot analyses were performed as previously described [23].

Where indicated, the cells were incubated for a set time in the dark with HY (0.5–2.5 μM). Irradiation for the cell photosensitization was done using a halogen lamp delivering 1.5–3 J/cm^2 in the visible range over 2–4 min. The irradiated cells were then centrifuged and resuspended in culture medium before being stained with the appropriate fluorescent probe and subjected to flow cytometric analysis. It should be noted that the fluorescence of the different probes that we used at the cellular level did not overlap that of HY ($\lambda_{em} > 600$ nm).

2.3. Analysis by flow cytometry

2.3.1. Intracellular pH. pHi was measured using a modification of Thomas' method[24]. JKV cells were loaded with 10 μM BCECF-AM (the membrane-permeable acetoxy methyl ester derivative of BCECF) by incubation in HBSS for 20 min at 37°C. Cells were then collected by centrifugation and washed once before being resuspended in HBSS containing 20 mM HEPES (pH 7.4). Flow cytometry was then immediately performed over 10 000 events using a Coulter Elite flow cytometer with dual laser excitation at 458 and 488 nm and a 530 ± 30 nm band pass filter for detection. Because the absorption spectrum of the probe is pH-dependent, the system makes it possible to monitor intracellular acidification by measurement of the fluorescence emission intensity ratio (λ_{em} = 535 nm) when the dye is excited at 488 nm versus the emission intensity when excited at 457 nm.

2.3.2. $\Delta\psi_m$. Cells were incubated for 15 min with 40 nM $DiOC_6(3)$. When used at a low concentration (< 0.5 μM), this carbocyanine dye specifically stains the mitochondria of live cells [25]. Changes of $\Delta\psi_m$ can be inferred from the fluorescence intensity because the electrophoretic accumulation of this cationic dye in mitochondria is governed by the Nersnt equation. Flow cytometric analysis was performed using excitation at 488 nm.

2.3.3. Measurements of caspase-3 activation. The cell-permeable fluorogenic substrate (PhiPhilux G1D2, OncoImmunin, INC Kensington, MD, USA) containing the sequence GDEVDG was used to detect caspase-3-like activity in intact cells by flow cytometry. Treated cells (1.5–3 J/cm^2 irradiation following 1 h incubation with 0.5–2.5 μM HY) were harvested and washed twice in phosphate-buffered saline (PBS). 10^6 cells were resuspended in 25 ml of substrate solution and incubated in the dark for 45 min at 37°C. After incubation, cells were washed and the fluorescence emission of fluorescein marker was measured at 530 ± 30 nm (FL1).

2.3.4. Measurement of the aberrant exposure of phosphatidyl serine residues. In non-apoptotic cells, PS residues are located on the inner leaflet of the plasma membrane. Entry into apoptosis causes them to be translocated to the extracellular side. Thus, the appearance of PS on the extracellular side can be exploited as a marker of apoptotic cells. Annexin V-FITC, which specifically binds to exposed PS, is a fast, simple and reliable tool for detection and quantification of early stage apoptosis in single cells by flow cytometry using excitation at 488 nm.

2.3.5. Analysis of DNA content. Cells were fixed in 50% ethanol and stored at 4°C until analysis, when they were stained with PI (50 μg/ml), treated with RNase (10 μg/ml) and washed in PBS. Their DNA content was analyzed by flow cytometry using an excitation at 488 nm.

2.4. Confocal fluorescence imaging of calcein-1AM-loaded mitochondria

Intracellular mitochondria were stained specifically with calcein-1AM through Co^{2+} quenching of cytosolic calcein fluorescence, as previously described [26]. Adherent mouse fibroblasts (3T3) were used for these experiments. Cell culture samples were prepared as previously described [20]. Through the microscope (Nikon Optiphot-2), fluorescent cell images were recorded using a 60×1.4 NA oil immersion objective (Nikon). This microscope was equipped for epi-fluorescence illumination and included a high pressure mercury lamp for excitation (100 W), a 12 bit digital cooled Micromax CCD camera (Princeton Instruments, Trenton, NJ, USA) and standard fluorescein (λ_{exc} = 450–490 nm, λ_{em} = 520–570 nm) and rhodamine (λ_{exc} = 530–560 nm, $\lambda_{em} > 600$ nm) filter sets were used for specific detection of calcein and HY, respectively. Data were acquired and analyzed with IPlab software (Scanalytics, Fairfax, VA, USA).

3. Results

3.1. Photosensitization and intracellular acidification

Intracellular acidification of HY (2.5 μM, 1 h)-treated cells was seen immediately after irradiation (1.5 J/cm^2), as revealed by a decrease in the fluorescence emission ratio of BCECF when compared to control cells (data not shown). Non-irradiated HY-treated cells showed the same ratio as the control. This result confirms that the pHi decrease must be related to the photosensitizing properties of the drug, as previously reported for 3T3 mouse fibroblasts using the ratiometric fluorescent pH probe SNARF-1 [19]. Experiments performed with JK-Bcl-2 gave the same results as for JKV.

3.2. Alteration of $\Delta\psi_m$

The potential-sensitive cyanine dye $DiOC_6(3)$ was chosen as a fluorescent probe for measuring $\Delta\Psi_m$ by flow cytometry because its fluorescence spectrum does not overlap that of HY. The $DiOC_6(3)$ fluorescence intensity from the cell is pro-

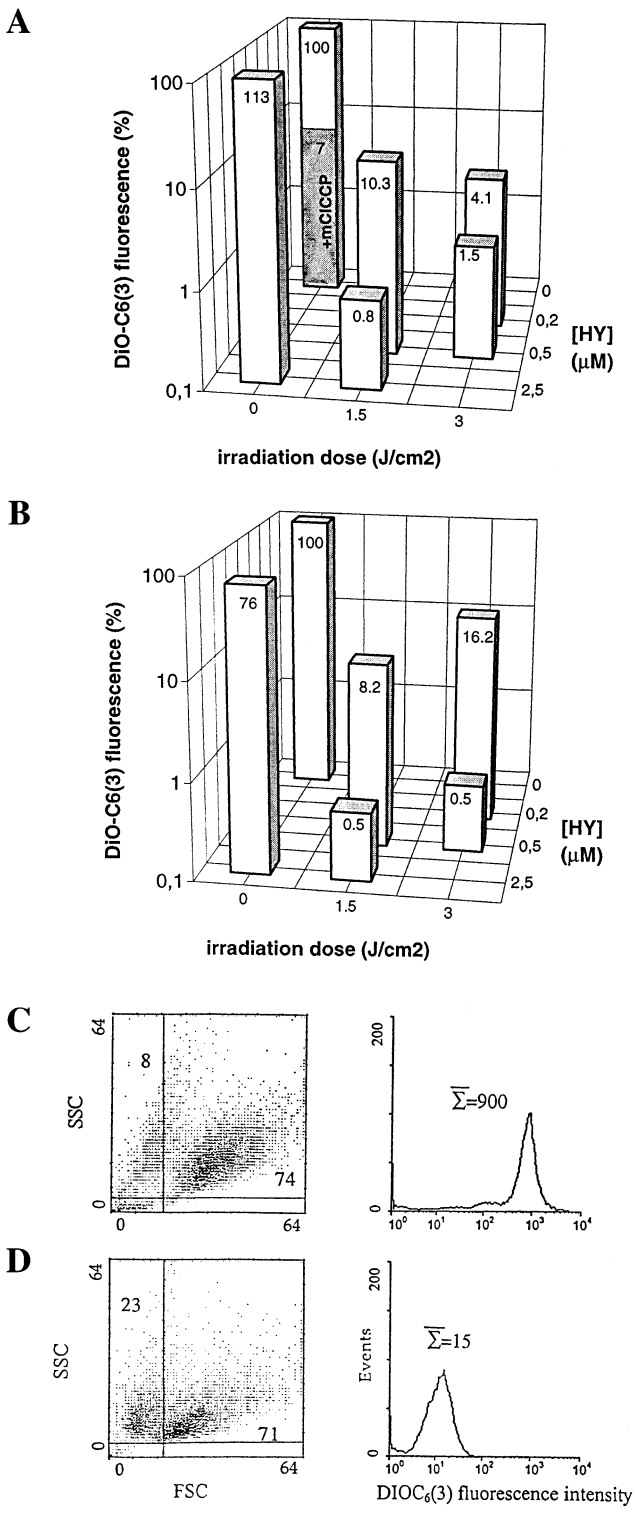

Fig. 1. Cytofluorimetric determination of the light dose and drug concentration-dependence of $\Delta\psi_m$ ($DiOC_6(3)$ fluorescence intensity) for (A) JKV cells, (B) JK-Bcl-2. Typical cytofluorimetric histograms and cell size (measured as forward scatter (FSC)) versus cell granulosity (measured as side scatter (SSC)) diagrams are given for (C) control cells and (D) JKV cells+0.5 μM HY+3 J/cm^2. The insert numbers (left top and right bottom of each graph) represent the respective percentages of the cell population.

portional to $\Delta\Psi_m$. As a control of $DiOC_6(3)$ uptake, cells were incubated with the protonophore mClCCP (50 μM, 15 min), a substance that dissipates $\Delta\Psi_m$. Comparing the fluorescence intensities of $DiOC_6(3)$ from control cells and HY-treated cells (Fig. 1), no effect can be detected without irradiation (2.5 μM HY for 1 h in the dark). On the other hand, a decrease in $DiOC_6(3)$ fluorescence intensity that is dependent on the light dose and drug concentration can be observed as early as 30 min after photosensitization (the minimum delay for $DiOC_6(3)$ incubation and cell preparation for flow cytometry). Over-expression of Bcl-2 did not protect cells from $\Delta\Psi_m$ dissipation. Moreover, pre-incubation of cells with CsA (10 μM) or BA (10 μM) did not affect our results (data not shown). Forward and side scattering analyses enable us to follow cell shrinkage. Two populations were distinguished in this way and expressed as a percentage of the total population (Fig. 1C). In the case of HY-treated cells, both exhibited a low $\Delta\psi_m$. Thus, $\Delta\psi_m$ appeared to precede cell shrinkage.

3.3. Imaging the mitochondrial membrane permeability

Membrane permeability of calcein-entrapped mitochondria has been monitored under a fluorescent microscope for HY-treated cells before (Fig. 2A) and after (Fig. 2B) irradiation (3 J/cm^2). The corresponding intracellular distribution of HY is also given (Fig. 2C,D). As shown in Fig. 2A, the addition of Co^{2+} during calcein loading enabled us to stain the mitochondrial compartment of the cell through specific quenching of cytosolic calcein fluorescence [26]. A comparison of Fig. 2A,C shows clear evidence that HY interacts with the mitochondrial compartment. After irradiation (Fig. 2B,C), mitochondrial-entrapped calcein almost disappeared while HY fluorescence gave the same pattern but with a lower intensity. Thus, HY photosensitization leads to (i) photobleaching of the drug and (ii) mitochondrial membrane permeability.

3.4. Aberrant exposure of the phosphatidyl serine residues at the plasma membrane level

Annexin V binding can be used to detect apoptosis before it becomes apparent through DNA strand breaks. As revealed by the percentages of annexin V positive cells observed 30 min and 2 h after irradiation (Fig. 3), HY is an as fast and powerful photo-inducer of apoptosis. The percentage of cell shrinkage correlates with the percentage of annexin V positive cells. In Jurkat cells which over-express Bcl-2 (JK-Bcl-2), the annexin positivity is substantially delayed when compared to Neo control cells (JKV).

3.5. Measurements of caspase-3 activation after photo-induction

Caspase-3 activation was successfully detected in a light dose and drug concentration-dependent manner as previously described for the $\Delta\Psi_m$ drop (Fig. 4I). Note that there is a close correlation between cell shrinkage and caspase-3 activation (Fig. 4C,D). The mitochondrial $\Delta\Psi_m$ drop (Fig. 4E,F) was followed by caspase-3 activation (Fig. 4G,H). The over-expression of Bcl-2 failed to inhibit caspase-3 activation but partially reduced it (by 10% as a mean value) (Fig. 4I).

3.6. Time course of the multiparametric analysis after photo-induction

The fraction of the cell population characterized by low

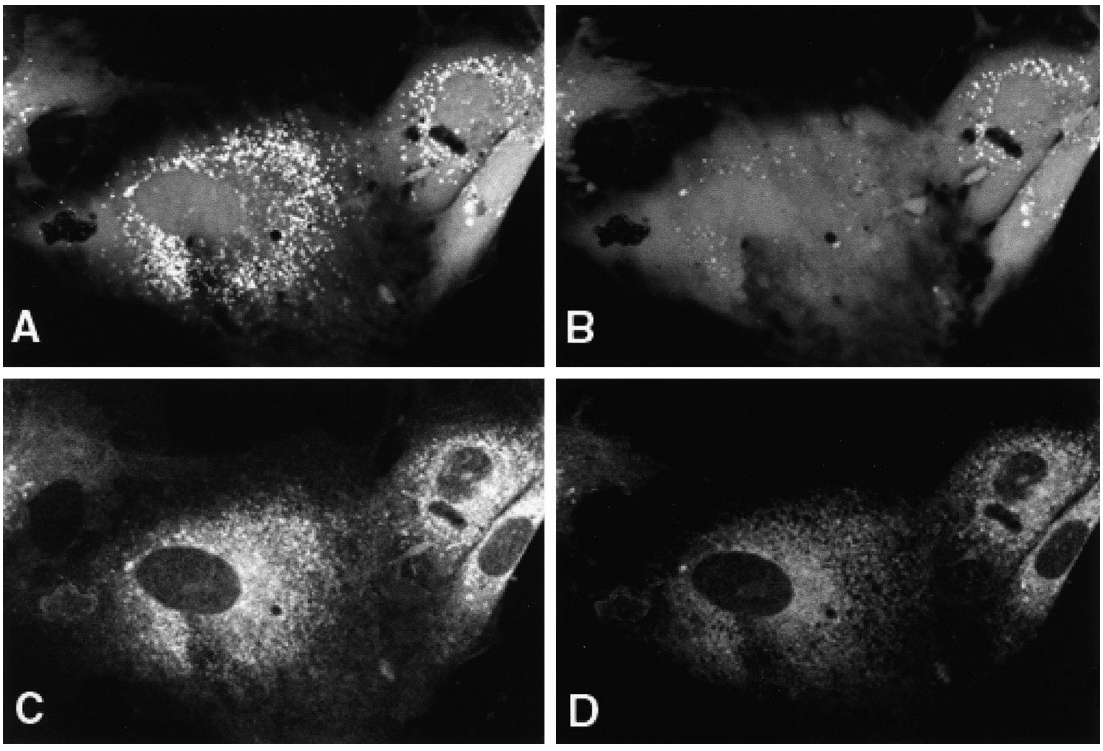

Fig. 2. Confocal fluorescence imaging of 3T3 mouse fibroblast pre-incubated with HY (1 h, 2.5 μM) and loaded for 15 min with 1 μM calcein-AM in the presence of 1 mM $CoCl_2$. (A and B) Calcein green fluorescence obtained before (A) and after (B) irradiation (3 J/cm^2). (C and D) Corresponding HY red fluorescence obtained before (C) and after (D) irradiation.

$\Delta\Psi_m$, annexin V positive staining and shrinkage is all displayed as a function of the post-irradiation time for JKV (A) or JK-Bcl-2 (B) cells treated with HY (Fig. 5). The hypoploid DNA fraction (see insert Fig. 5) is also displayed for the 2 h post-irradiation time. $\Delta\Psi_m$ depolarization for both cell lines can be immediately observed after photosensitization. The time necessary for sample preparation staining enabled us to obtain the first measurement 30 min after irradiation. Annexin V staining and cell shrinkage were then observed in parallel. Bcl-2 over-expression delayed these processes and lead to a lower fraction of hypoploid DNA cell contents. In all cases, the percentage of cells with hypoploid DNA was lower than the percentage of annexin V positive cells. This is in agreement with the view that PS residue exposure is an early event which precedes nuclear DNA cleavage. However, a significant fraction of the JKV cell population was characterized by hypoploid quantities of DNA, while results obtained with JK-Bcl-2 cells indicated a protective effect of Bcl-2 expression on DNA cleavage.

4. Discussion

Singlet oxygen production, hydroxyl radical generation and local acidification have already been described as the events occurring during HY cell photosensitization [4,17,19,27]. Nuclear alteration characteristic of apoptosis has also been observed after HY cell photosensitization [14], as well as procaspase-3 activation [15]. To evaluate how the primary photoprocesses can lead to nuclear apoptosis, we studied mitochondria. It has recently been suggested that mitochondria are the key targets of oxygen-dependent HY phototoxicity in cells [12]. $\Delta\Psi_m$ reduction and subsequent superoxide anion production have been observed in the early stages of programmed cell death [28,29]. The present results indicate that HY cell photosensitization induces an almost instantaneous dissipation of $\Delta\Psi_m$ and cytoplasmic acidification which precede the entry of the whole cell population into apoptosis. The decrease of $\Delta\Psi_m$ and apoptosis both appear to be tightly dependent on the drug concentration and on the dose of light irradiation. Moreover, the $\Delta\Psi_m$ drop occurred not only in cells which exhibited a typical cell shrinkage but also in cells which showed no changes in morphology and would usually have been considered as non-apoptotic. This observation is in full agreement with the fact that $\Delta\Psi_m$ collapse has been reported as an early event in the apoptotic process [16,28]. The marked dissipation of $\Delta\Psi_m$ following photosensitization led us to focus on the eventual involvement of the mitochondrial permeability transition (MPT) pore, which is a potential effector of mitochondrial swelling, and the subsequent release of apoptogenic factors from the mitochondrial intermembrane space [30]. It is known that the MPT pore is activated by oxidants [31] and that HY is among the most efficient reagents for generating singlet oxygen ($^1O_2$) and promoting superoxide anion ($O_2^{\bullet -}$) in model and cellular systems [27,32]. However, pre-treatment of cells with CsA or BA, reported to be specific inhibitors of the MPT pore both on isolated mitochondria and in whole cells [26,31], does not protect cells from mitochondrial membrane depolarization in our study. Thus, the opening of MPT pores does not seem to be directly involved in the $\Delta\psi_m$ dissipation process which was photo-induced by HY. Nevertheless, as revealed by the intracellular redistribution of the fluorescent calcein fluid marker from the mitochondria to the cytosol after irradiation, HY photosensitization clearly induces mitochondrial permeability. HY may thus

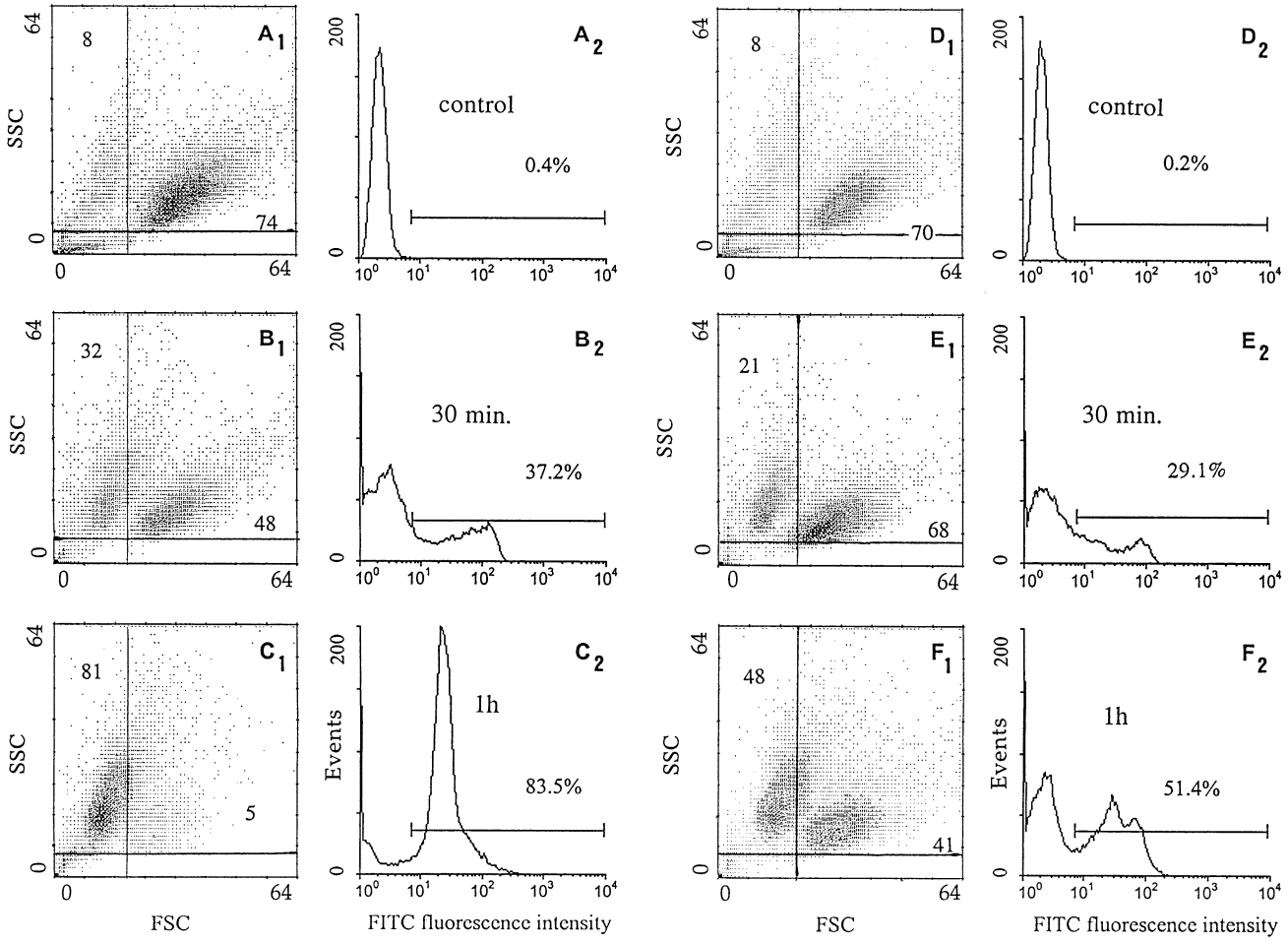

Fig. 3. Post-irradiation time course of annexin V-FITC binding (right) and cell shrinkage (left) obtained after photosensitization with HY (1 h incubation with 2.5 μM HY and 3 J/cm^2 irradiation). (A) JKV control cells. (B and C) JKV cells 30 and 60 min after irradiation, respectively. (D) JK-Bcl-2 control cells. (E and F) JK-Bcl-2 cells 30 and 60 min after irradiation, respectively. The insert numbers (left top and right bottom of each graph) represent the respective percentages of the cell population.

act directly at the level of the mitochondrial membrane through non-specific alterations of its integrity, as we have previously described for the plasma membrane [33]. Under our experimental conditions (1.5–3 J/cm^2 irradiation following 1 h incubation with 0.5–2.5 μM), over-expression of the anti-apoptotic protein Bcl-2 did not protect cells from the $\Delta\psi_m$ decrease induced by HY photosensitization. However, it did delay the subsequent annexin V binding, cell shrinkage and reduced caspase-3 activation as well as the fraction of cells which were hypoploid 2 h after irradiation. The apoptotic induction pathway triggered by HY photosensitization therefore does not appear to be totally independent of *bcl-2* expression, in contrast to what was stated for glioma cells expressing a high level of *bcl-2* [14]. Indeed, previous studies have already described that Bcl-2 could block apoptosis at a point downstream of the collapse of the cellular energy metabolism and prolongs cell survival after cytochrome *c* release [34–38]. Authors suggest that Bcl-2 could regulate caspase activity as well as the positive feed back of caspase-3 on cytochrome *c* release downstream mitochondria. Moreover, Bcl-2 is not only localized to the mitochondrial membrane but also takes a place in the endoplasmic reticulum and nuclear envelope. Indeed, the ability of Bcl-2 to suppress cell death through inhibition of nuclear import of induced wild-type p53 protein has been reported [39]. Bcl-2 targeted to the endoplasmic reticulum can also inhibit Myc-induced apoptosis in the rat-1 fibroblasts [40]. In this context, the partially protective effect of Bcl-2 for HY-induced apoptosis observed in our study can be interpreted as the consequence of a direct interaction of Bcl-2 with cytosolic cytochrome *c* previously released from mitochondria upon $\Delta\psi_m$ decrease and/or Bcl-2 inhibition of the deleterious retro-effect of caspase-3 on the mitochondrial permeability transition pore and/or mitochondrial membrane components such as Bcl-2 itself. However, differences in the percentage of hypoploid DNA are the most significant differences between JKV and JK-Bcl-2 HY-treated cells. Thus, a possible role of Bcl-2 localized at the nuclear membrane should be taken into account.

5. Conclusion

Experimental data on lactate dehydrogenase leakage, lipid peroxidation and protein oxidation assays have been obtained by studying HY phototoxicity and its effect on mitochondrial energy in EMT6 mouse mammary carcinoma cells [12]. Our results suggest that the dual effects of oxidative damage and the change in intracellular pH elicited by photo-activated HY could be the combination which makes this drug one of the

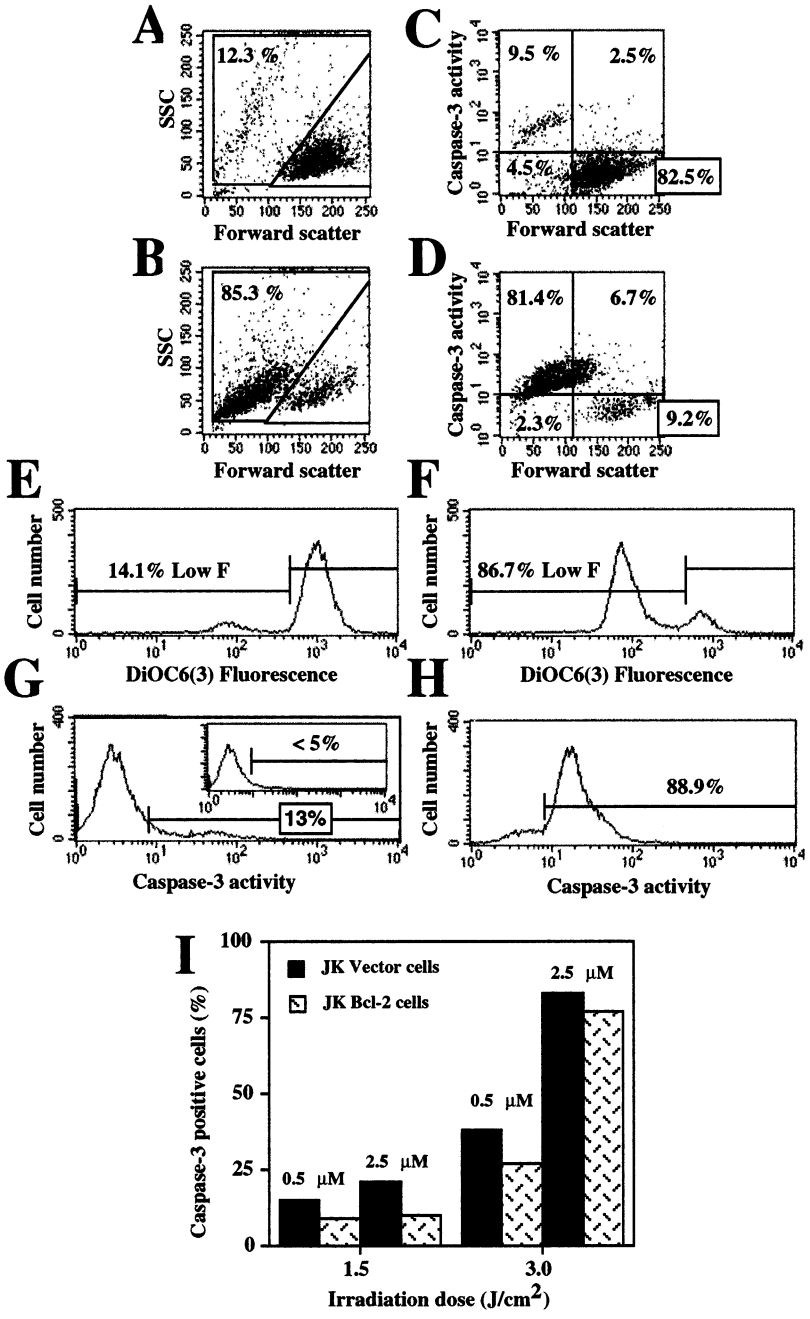

Fig. 4. Measurements of caspase-3 activation by flow cytometry. Cells were first incubated for 1 h with either 0.5 or 2.5 μM HY and then kept in the dark or post-irradiated with 1.5 or 3 J/cm^2 before the staining procedure (see Section 2). Biparametric histograms represent the light scattering properties of JKV (A, B), the light scatter and the caspase-3 activity (C, D) in the case of JKV cells treated with 2.5 μM HY and 3 J/cm^2. The $\Delta\psi_m$s (E, F) and the caspase-3 activity (G, H) are represented as monoparametric histograms (insert in G corresponds to the cell population in A which exhibit a high forward scatter, i.e. intact control cells). The caspase-3 activations in Jurkat-Neo cells and in Jurkat-Bcl-2 cells are presented in the context of a different HY concentration (0.5 and 2.5 μM) and post-irradiation doses (1.5 and 3 J/cm^2) (I).

most powerful photodynamic agents in nature. We also suggest that oxygen-dependent HY phototoxicity can act on mitochondria at a cellular as well as a sub-cellular level. We conclude that the mitochondrial membrane should be considered as a key intracellular target accounting for the cellular phototoxicity of HY, that the induction of apoptosis appears to be triggered by photo-induced alterations of mitochondrial function leading to $\Delta\psi_m$ collapse and that the MPT pore is not directly involved in the dissipation of $\Delta\psi_m$. However, our results give evidence for a mitochondrial downstream effect of Bcl-2 in the apoptotic pathway. Finally, the rapid apoptosis photo-induced by these drugs is probably related to their hydrophobic nature and to their ability to promote a high level of oxidants and intracellular acidification. Thus, apoptosis involving alterations of mitochondrial function alterations appears to be an essential process in HY cellular phototoxicity and accounts for its anti-neoplastic activity.

Acknowledgements: This work was supported by Grant no. 9570 from the 'Association pour la Recherche sur le Cancer'.

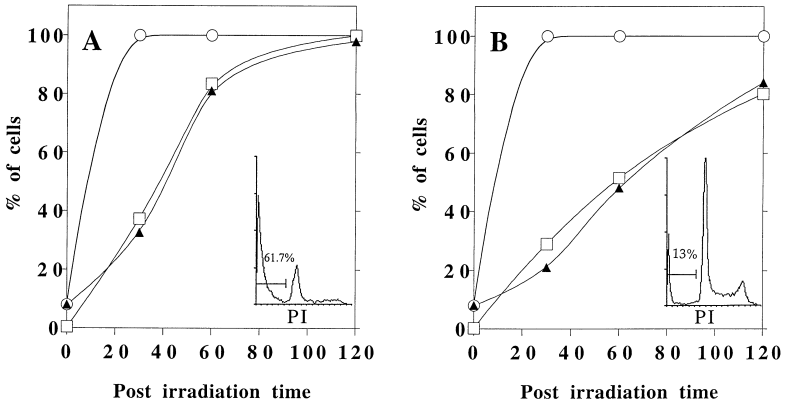

Fig. 5. Fractions of the cell population characterized by a low $\Delta\Psi_m$ (○), annexin V positive staining (□) and shrinkage (▲) as a function of the post-irradiation time for HY-treated cells: (A) JKV, (B) JK-Bcl-2. Insert: DNA content analysis (PI fluorescence) determined for 2 h post-irradiation time (horizontal bar corresponds to the region of the hypoploid fraction).

References

[1] Pace, N. and Mackinney, G. (1941) J. Am. Chem. Soc. 63, 2570–2574.
[2] Carpenter, S. and Kraus, G. (1991) Photochem. Photobiol. 53, 169–174.
[3] Lenard, J., Rabson, A. and Vanderoef, R. (1993) Proc. Natl. Acad. Sci. USA 90, 158–162.
[4] Thomas, C. and Pardini, R. (1992) Photochem. Photobiol. 55, 831–837.
[5] Andreoni, A., Colasenti, A., Colasanti, P., Mastrocinque, M., Riccio, P. and Roberti, G. (1994) Photochem. Photobiol. 59, 529–533.
[6] Vandenbogaerde, A., Geboes, K., Cuveele, J., Agostonis, P., Merlevede, W. and de Witte, P. (1996) Anticancer Res. 16, 1619–1626.
[7] Vandenbogaerde, A., Delaey, E., Vantieghem, A., Himpens, B., Merlevede, W. and de Witte, P. (1998) J. Photochem. Photobiol. 67, 119–125.
[8] Diwu, Z., Zimmerman, J., Meyer, T. and Lown, J. (1994) Biochem. Pharmacol. 47, 373–385.
[9] Utsumi, T., Okuma, M., Kanno, T., Yasuda, T., Kobuchi, H., Horton, A. and Utsumi, K. (1995) Arch. Biochem. Biophys. 316, 493–497.
[10] De Witte, P., Agostinis, P., Van Lint, J., Merlevede, W. and Vandenheede, J. (1993) Biochem. Pharmacol. 46, 1929–1936.
[11] Utsumi, T., Okuma, M., Kanno, T., Takehara, Y., Yoshioka, T., Fujita, Y., Horton, A. and Utsumi, K. (1995) Biochem. Pharmacol. 50, 655–662.
[12] Johnson, S., Dalton, A. and Pardini, R. (1998) Free Radic. Biol. Med. 25, 144–152.
[13] Miccoli, L., Beurdeley-Thomas, A., De Pinieux, G., Sureau, F., Oudard, S., Dutrillaux, B. and Poupon, M. (1998) Cancer Res. 58, 5777–5786.
[14] Weller, M., Trepel, M., Grimel, C., Schabet, M., Bremen, D., Krajewski, S. and Reed, J. (1997) Neurol. Res. 19, 459–470.
[15] Vantieghem, A. et al. (1998) FEBS Lett. 440, 19–24.
[16] Zamzami, N. et al. (1995) J. Exp. Med. 182, 367–377.
[17] Diwu, Z. (1995) Photochem. Photobiol. 61, 529–539.
[18] Fehr, M., Mc Closkey, A. and Petrich, J. (1995) J. Am. Chem. Soc. 117, 1833–1836.
[19] Sureau, F., Miskovsky, P., Chinsky, L. and Turpin, P. (1996) J. Am. Chem. Soc. 118, 9484–9487.
[20] Chaloupka, R., Sureau, F., Kocisova, E. and Petrich, J. (1998) Photochem. Photobiol. 68, 44–50.
[21] Bielski, B., Ravindra, L. and Sutherland, M. (1983) J. Biol. Chem. 258, 4759–4761.
[22] Gottlieb, R., Nordberg, J., Skowronski, E. and Babior, B. (1996) Proc. Natl. Acad. Sci. USA 93, 654–658.
[23] Aillet, F. et al. (1998) J. Virol. 72, 9698–9705.
[24] Thomas, J., Buschbaum, R., Zimniak, A. and Racker, E. (1979) Biochemistry 18, 2210–2218.
[25] Witkowski, J. and Micklem, H. (1985) Immunology 53, 307–313.
[26] Petronilli, V., Miotto, G., Canton, M., Brini, M., Colonna, R., Bernardi, P. and Di Lisa, F. (1999) Biophys. J. 76, 725–734.
[27] Ehrenberg, B., Anderson, J. and Foote, C. (1998) Photochem. Photobiol. 68, 135–140.
[28] Vayssière, J., Petit, P., Risler, Y. and Mignotte, B. (1994) Proc. Natl. Acad. Sci. USA 91, 11752–11756.
[29] Green, R. and Reed, J. (1998) Science 281, 1309–1312.
[30] Susin, S. et al. (1999) Nature 397, 441–446.
[31] Zoratti, M. and Szabo, I. (1995) Biochim. Biophys. Acta 1241, 139–176.
[32] Hadjur, C. and Jardon, P. (1995) J. Photochem. Photobiol. B Biol. 29, 147–156.
[33] Chaloupka, R., Obsil, T., Plasek, M. and Sureau, F. (1999) Biochim. Biophys. Acta 1408, 39–47.
[34] Bossy-Wetzel, E. and Green, D. (1999) J. Biol. Chem. 274, 17484–17490.
[35] Marton, A., Mihalik, R., Bratincsak, A., Adleff, V., Petak, I., Vegh, M., Bauer, P. and Krajcsi, P. (1997) Eur. J. Biochem. 250, 467–475.
[36] Rosse, T., Olivier, R., Monney, L., Rager, M., Conus, S., Fellay, I., Jansen, B. and Borner, C. (1998) Nature 391, 496–499.
[37] Cosulich, S., Savory, P. and Clarke, P. (1999) Curr. Biol. 9, 147–150.
[38] Carthy, C., Granville, D., Jiang, H., Levy, J., Rudin, C., Thompson, C., McManus, B. and Hunt, D. (1999) Lab. Invest. 79, 953–965.
[39] Beham, A. et al. (1997) Oncogene 15, 2767–2772.
[40] Lee, S., Hoeflich, K., Wasfy, G., Woodgett, J., Leber, B., Andrews, D., Hedley, D. and Penn, L. (1999) Oncogene 18, 3520–3528.